131 POLARIMETRIC RADAR CHARACTERISTICS OF WARM FRONT-CROSSING STORMS ON 9 APRIL 2015

Cynthia A. Van Den Broeke
Lincoln, NE
Matthew S. Van Den Broeke*
University of Nebraska – Lincoln, Lincoln, NE

1. INTRODUCTION

Convective storms encountering a pre-existent thermal boundary may also encounter large moisture and instability gradients, and local maxima in horizontal and vertical vorticity. Past studies have noted a relationship between storm-boundary interactions and tornado production. Maddox et al. (1980) documented several cases where tornado production was confined primarily to storms that interacted with thermal boundaries, such as warm fronts, outflow boundaries, and stationary fronts. At least two of the thermal boundaries were reinforced by cooling from nearby Great Lakes. Weaver and Nelson (1982) observed a tornado develop at the intersection of two outflow boundaries. Rogash and Smith (2000) noted that the strongest tornadoes in the 1 March 1997 severe weather outbreak tended to occur near an outflow boundary. There was also substantial flash flooding in the vicinity of the same boundary. Markowski et al. (1998) noted that 70% of tornadoes in their VORTEX-95 dataset (made up mostly of tornadoes of F2 or greater intensity) occurred near a surface boundary, with most occurring on the cold side of the boundary. Rasmussen et al. (2000) specifically examined the 2 June 1995 tornado outbreak and noted that only supercells that crossed or developed on the cold side of an outflow boundary were tornadic. While Maddox et al. (1980) suggested that vertical vorticity along thermal boundaries was a significant source of vorticity for tornadic storms, Rogash and Smith (2000) and Rasmussen et al. (2000) instead suggested baroclinically-generated horizontal vorticity may have been a more significant source of low-level vorticity. With the exception of flooding, association of other types of severe weather with storm-boundary interactions has not been as widely researched.

On 9 April 2015, a warm front moved northward across Illinois, eventually becoming quasi-stationary over northern Illinois. Numerous convective storms initiated south of the frontal boundary. Several of these storms moved northeast and crossed the frontal boundary over far northern Illinois (Fig. 1). The focus of this case study was on three of these storms: two anticyclonic supercells (Storms 1 and 2) and one cyclonic, tornadic supercell (Storm 3). This case study focuses on microphysical and updraft characteristics of these storms as they cross the frontal boundary.

2. METHODOLOGY

Initially, radar, satellite, and surface observations were consulted to estimate the surface location of the front. There was no radar fine line associated with the front, and extensive cloud cover made the use of visible satellite imagery futile, so the frontal position was estimated using surface observations alone. Given the wide geographic spacing between stations, uncertainty in the location of the surface frontal boundary may have been as much as 30 km, but was likely less due to temporal continuity of boundary position.

Level II data from three Weather Surveillance Radar – 1988 Doppler weather radars were used to analyze storm structure and inferred microphysical properties: Davenport, IA (KDVN), Chicago, IL (KLOT), and Milwaukee, WI (KMKX). The data mainly cover the time between 2200 UTC and 0100 UTC.

**Corresponding author address*: Matthew S. Van Den Broeke, 306 Bessey Hall, Lincoln, NE 68588-0340.
E-mail: mvandenbroeke2@unl.edu

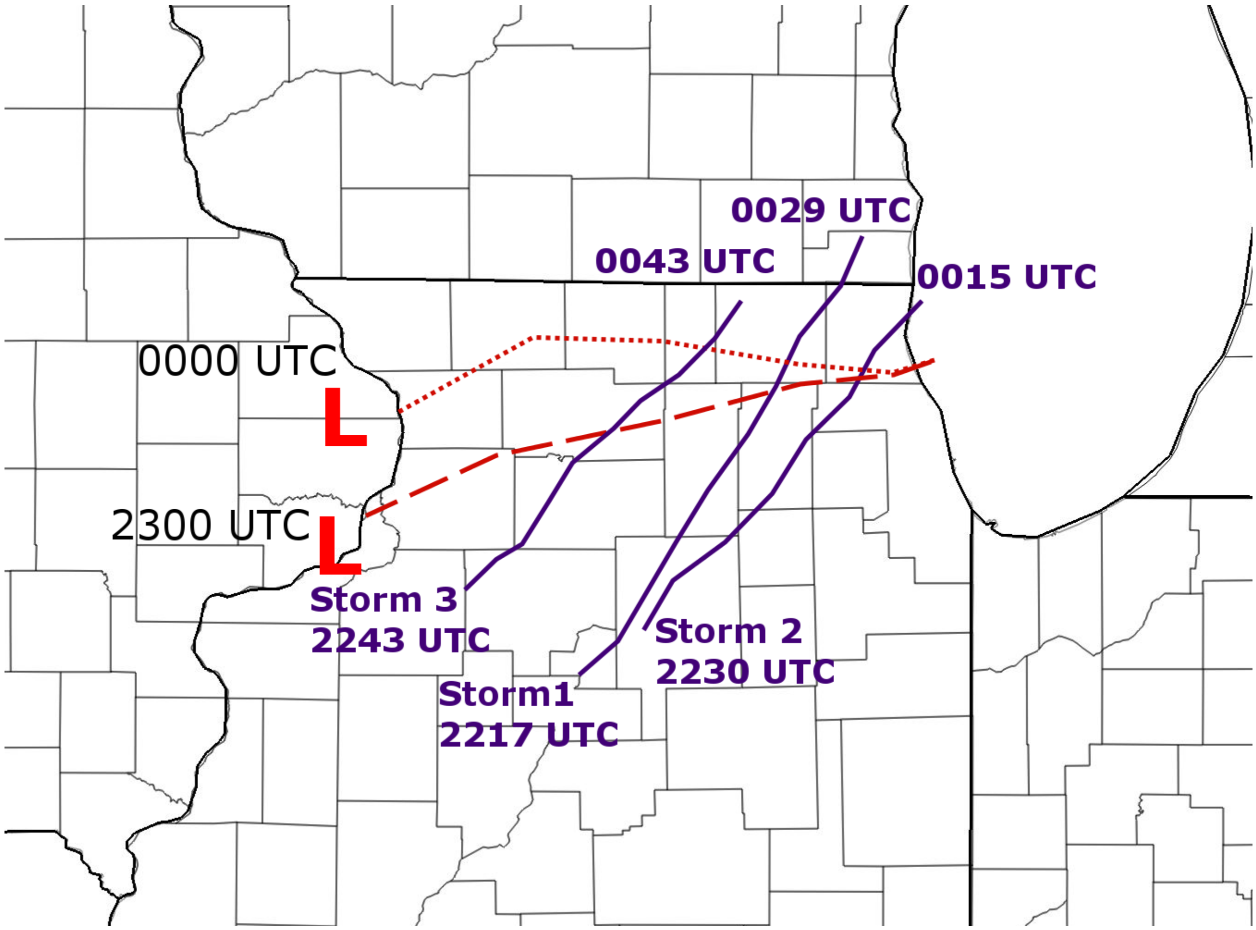

Fig. 1. Storm tracks (purple) for three supercells that crossed a surface frontal boundary on 9 April 2015 with position of low indicated by large, red “L.” Approximate position of front at 2300 UTC is dashed; position at 0000 UTC is dotted. Map courtesy Oklahoma Climatological Survey.

Level III data were unavailable for most of this time period, so specific differential phase (K_{DP}) was not included in the analysis. Updraft characteristics observed included height of the 1-dB Z_{DR} column, maximum heights of the 50 dBZ and 60 dBZ echo, and presence of a weak echo region (WER) or bounded weak echo region (BWER). Maximum velocity difference, or the difference between the maximum outbound and inbound velocity, was used as one measure of mesocyclone strength. For the anticyclonic supercells (Storms 1 and 2), velocity difference was measured as close to 3 km ARL as possible since neither storm produced a low-level mesocyclone. Velocity difference was calculated for the lowest elevation angle for Storm 3. In addition, characteristics of the Z_{DR} arc at 0.5° if below 1.5 km ARL, and of the hail signature throughout the depth of the storm were noted. Evolution of these traits was compared with reports of severe weather and the location of the storm relative to the surface front. Reports of severe weather were obtained through the National Climatic Data Center (NCDC) Storm Events Database.

3. SYNOPTIC AND MESOSCALE ENVIRONMENT

At 1200 UTC on 9 April, the warm front stretched across central Illinois with an area of low pressure over far south-central Iowa (all times are

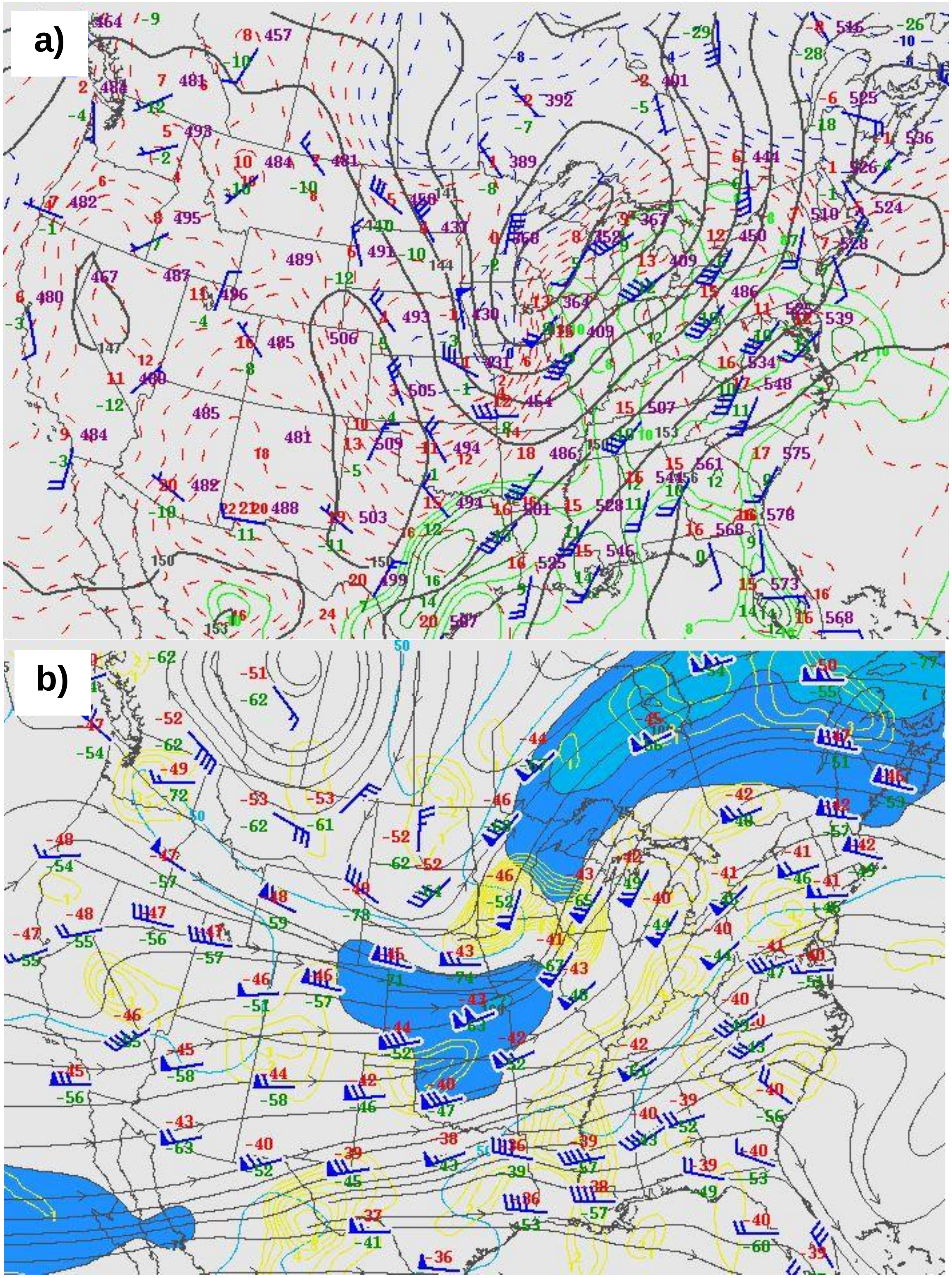

Fig. 2. 10 April 2015 0000 UTC a) 850 hPa wind (half barb 5 kt, whole barb 10 kt, and flag 50 kt), temperature (red dashed lines for T > 0°C, blue dashed lines for T < 0°C) dewpoint temperature (°C, green contours) and height (solid black lines). b) 300 hPa streamlines, wind (kt) and divergence (yellow contours). Courtesy Storm Prediction Center.

in UTC). Warm advection and moderate southwest flow at 850 hPa were present over northern Illinois. A 28 m s^{-1} (55 kt) jet was located on the south side of the 850 hPa low, and moved into far eastern Iowa by 0000 on 10 April (Fig. 2a). At 300 hPa, a sharp trough was positioned over the northern High Plains, with an attendant 41 m s^{-1} (80 kt) jet streak over central Nebraska. By 0000, the trough had progressed to the central to eastern Dakotas (Fig. 2b). Two jet streaks were evident: the first to the northeast of the trough from Minnesota northeastward through Hudson Bay and eastward to eastern Canada, and the second from western Kansas and Nebraska through far eastern Kansas. An attendant area of 300 hPa divergence was situated over eastern Iowa, northwest Illinois, and southwest Wisconsin (Fig. 2b). Low-level moisture advection brought an increase in surface dewpoint temperatures across northern Illinois, from 6-8°C at 1200 to 14-18°C by 2200. South of the front, SBCAPE was over 2000 J kg^{-1} by 0000, while 0-6 km shear was 23 m s^{-1} (45 kt) at 1800, increasing to 28 m s^{-1} (55 kt) by 0000 across central Illinois (not shown). Over far eastern Iowa, ahead of the low, the 0-6 km shear was lower at 1800 (15 m s^{-1}, or 29 kt), increasing to 34 m s^{-1} (67 kt) by 0000, behind the low, which had moved to the north-northeast of the site (not shown). Thus, the environment was supportive of supercell development.

Two of the storms of interest originated just after 2200 in north-central Illinois as anticyclonic members of storm splitting (Storms 1 and 2, see Fig. 1). The third storm (Storm 3) was a cyclonically-rotating, tornadic supercell that initiated farther west. These storms all moved rapidly northeast and interacted with the surface front between 2300 and 0030.

3. RESULTS

3.1 Anticyclonic Storms 1 and 2

Storms 1 and 2 moved nearly parallel to each other toward the northeast and crossed the surface front between 2345 and 2354. Both supercells produced one inch diameter hail during their encounter with the frontal boundary, with Storm 1 producing two more reports of 0.88 inch diameter hail as it moved to the cold side of the front (Fig. 3). Otherwise, there were no severe or near-severe weather reports from either storm. Neither supercell produced a low-level mesocyclone.

The structural and updraft evolution of Storm 1 reflected a decrease in intensity beginning just before it encountered the boundary. Storm 1 rapidly strengthened between 2301 and 2320, with an increase in the maximum height of the 50 dBZ core from 4.65 km ARL to over 8 km ARL. The maximum altitude of the 60 dBZ core was more irregular, but it also showed a general increase through 2315 (Fig. 4a). At the same time, a three-body scatter spike (TBSS) and lowered co-polar cross-correlation coefficient (ρ_{hv}) values aloft, beginning around 2311, indicated the development of a hail core. A BWER developed by 2325, and an inflow notch appeared on the north side of the storm, near the surface, at the same time. Maximum velocity difference in the mesocyclone near 3 km ARL also increased through 2325 (Fig. 4a). The storm began a brief decline around 2340, marked by a decrease in the 50 dBZ core height. The TBSS became indistinct and intermittent, and low ρ_{hv} began to appear at 0.5°, perhaps indicating the beginning of hail fallout. Maximum height of the 60 dBZ echo had begun a decrease approximately 10 minutes earlier, at 2330. The storm still sustained a BWER, but maximum velocity difference also briefly decreased beginning around 2345. This apparent decrease in intensity was followed by reports of hail at the surface, which occurred very near the location of the surface front. Storm 1 briefly seemed to recover intensity, with an increase in maximum 50 and 60 dBZ height, but it finally declined as it moved farther into the cold air on the north side of the front. Despite the decline as the storm interacted with the front, it was at this time that the inflow notch was most distinct (see Fig. 5).

Storm 2 followed similar initial development, with an increase in maximum 50 and 60 dBZ height as the storm matured south of the front, and then a decrease in intensity with hail fallout near the front (Fig. 4b). Unlike Storm 1, maximum 60 dBZ height in Storm 2 began to decrease just after 2320, well before the interaction with the surface front. Maximum

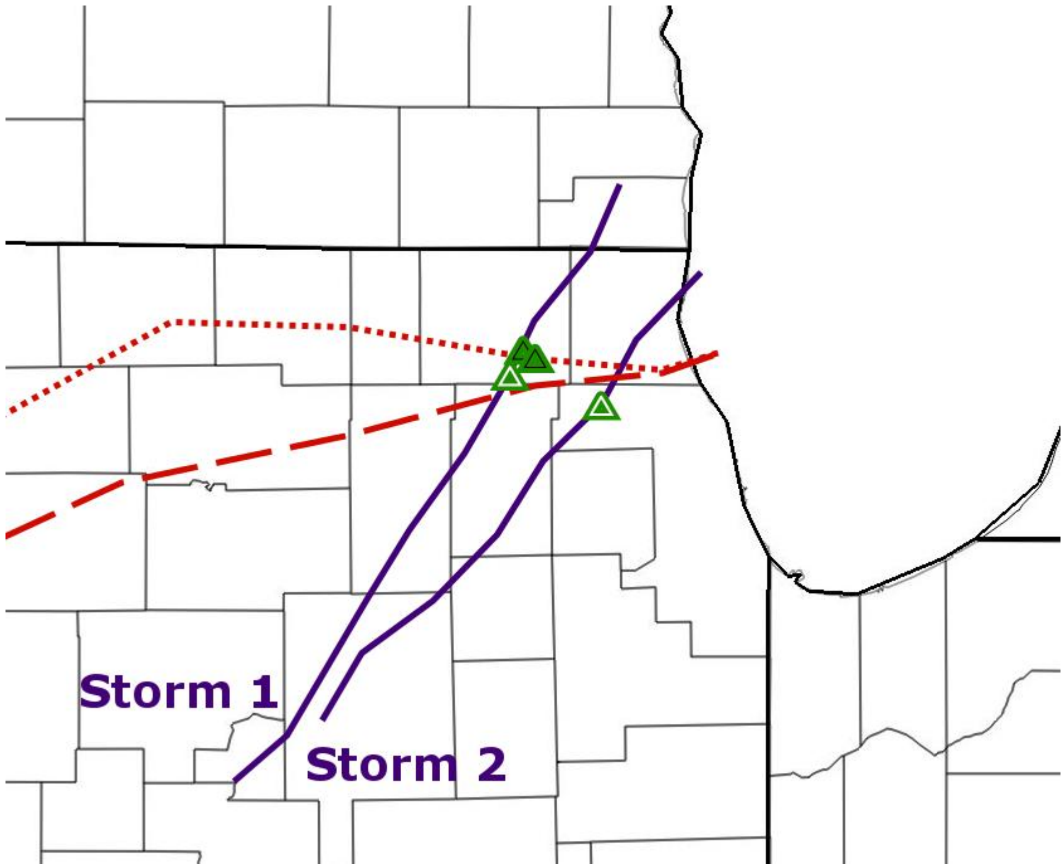

Fig. 3. Paths of Storms 1 and 2 (purple) with hail reports. Hail 1 inch in diameter indicated by a green-and-white triangle, and 0.88 inch diameter hail is indicated by a green-and-black triangle. Red dashed (dotted) line is location of front at 2300 UTC (0000 UTC). Map courtesy Oklahoma Climatological Survey.

velocity difference stayed nearly constant prior to 2345 when it abruptly began to decrease. Unlike Storm 1, Storm 2 did not recover or even briefly maintain constant intensity after crossing the front, but continued to decline until its demise just after 0015.

Z_{DR} column height did not seem to follow other indicators of storm intensity in Storm 2. However, in Storm 1, there was a slight increase in height as the storm intensified and a slight decrease just prior to the decline in intensity (Fig. 4a). Z_{DR} column height increased again as the storm crossed to the cold side of the boundary and briefly intensified. In Storm 2, Z_{DR} column height remained nearly constant even during the precipitous decline in storm intensity after the storm crossed the boundary (Fig. 4b).

One interesting change did take place in both supercells as they crossed the frontal boundary: the Z_{DR} arc became slightly broader with an increase in mean Z_{DR} values within the arc (Fig. 5). Two possibilities to explain this observation include (1) a difference in storm-relative wind in association with the boundary, or (2) evaporation of smaller drops as the storms encountered drier air at low-levels near the front. The northward motion of the storms across the boundary meant they moved from drier air (dewpoint depression of greater than 4°C) into a moister low-level air mass (dewpoint depression of 1.1°C or less), so the latter is probably not a factor in Z_{DR} arc evolution. It is therefore possible that much of the change in the appearance of the Z_{DR} arcs was a reflection of the storms encountering a different storm-relative wind profile near the boundary.

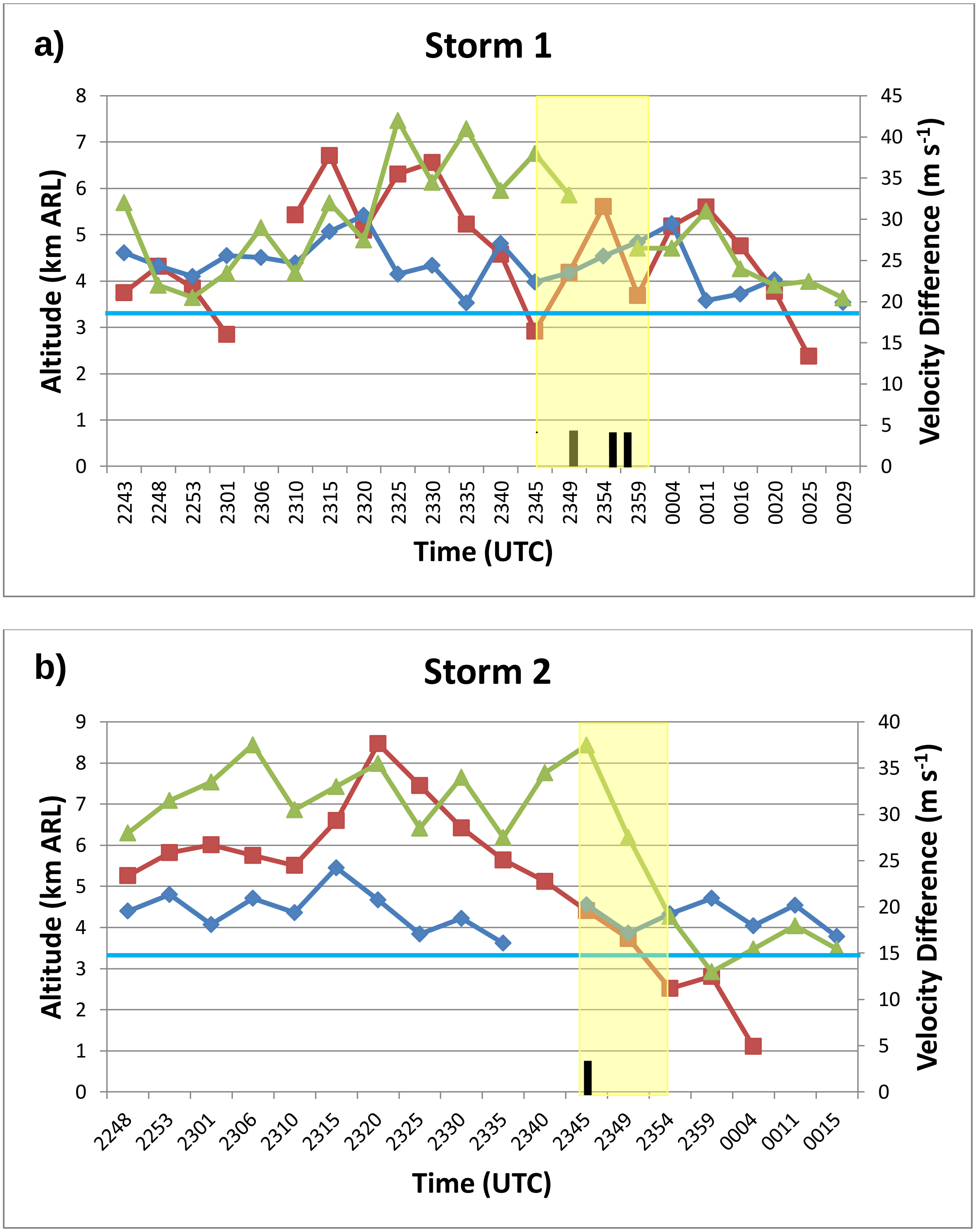

Fig. 4. Maximum height of 60 dBZ Z_{HH} (red line with squares) and top of the 1-dB Z_{DR} column (blue line with diamonds) with maximum velocity difference (green line with triangles) for a) Storm 1 and b) Storm 2. Horizontal, light blue line marks approximate ambient 0°C height. Vertical black lines at chart bottom are hail reports. Yellow box is approximate window of storm-boundary interaction.

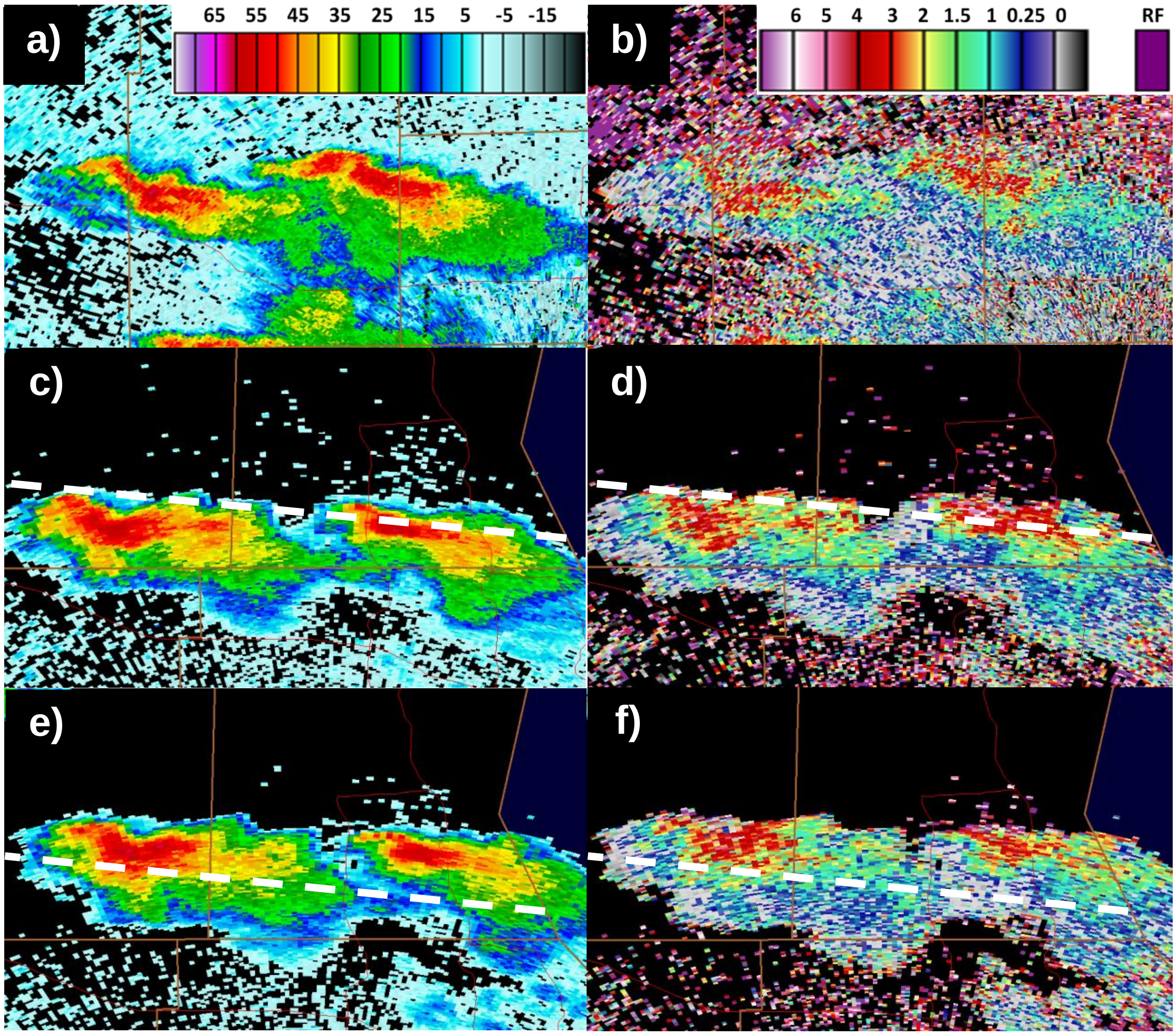

Fig. 5. Z_{HH} (left column) and Z_{DR} (right column) for Storms 1 and 2 at 2330 UTC (a, b), 2354 UTC (c, d), and 2359 UTC (e, f). Approximate location of front represented by white, dashed line.

3.2 Storm 3: Tornadic Supercell

Storm 3 was a cyclonically rotating supercell, and originated well south of the surface frontal boundary. This supercell produced six tornadoes, including one long-track, violent tornado. The only reports of hail from this storm occurred well south of the front and prior to the first tornado. Unlike Storms 1 and 2, there was not a cluster of severe weather reports in the vicinity of the quasi-stationary front. It is possible other severe weather was underreported while the significant tornado was in progress. The long-track tornado occurred while the supercell was south of the front, and one of the brief, weak tornadoes was a satellite tornado. This storm encountered the boundary from shortly before 0020 through 0030. The long-track tornado was already decaying as the storm approached the boundary, meeting its demise at 0020. There was another weak tornado toward the end of the lifespan of the long-track tornado, from 0015 through 0021. As the storm encountered the boundary and shortly thereafter, the storm produced a series of three additional weak tornadoes (Fig. 6). The reason for this shift from a violent, long-track tornado to production of several weak, short-lived tornadoes was unknown.

As with Storms 1 and 2, the Z_{DR} arc underwent a dramatic transformation as the storm

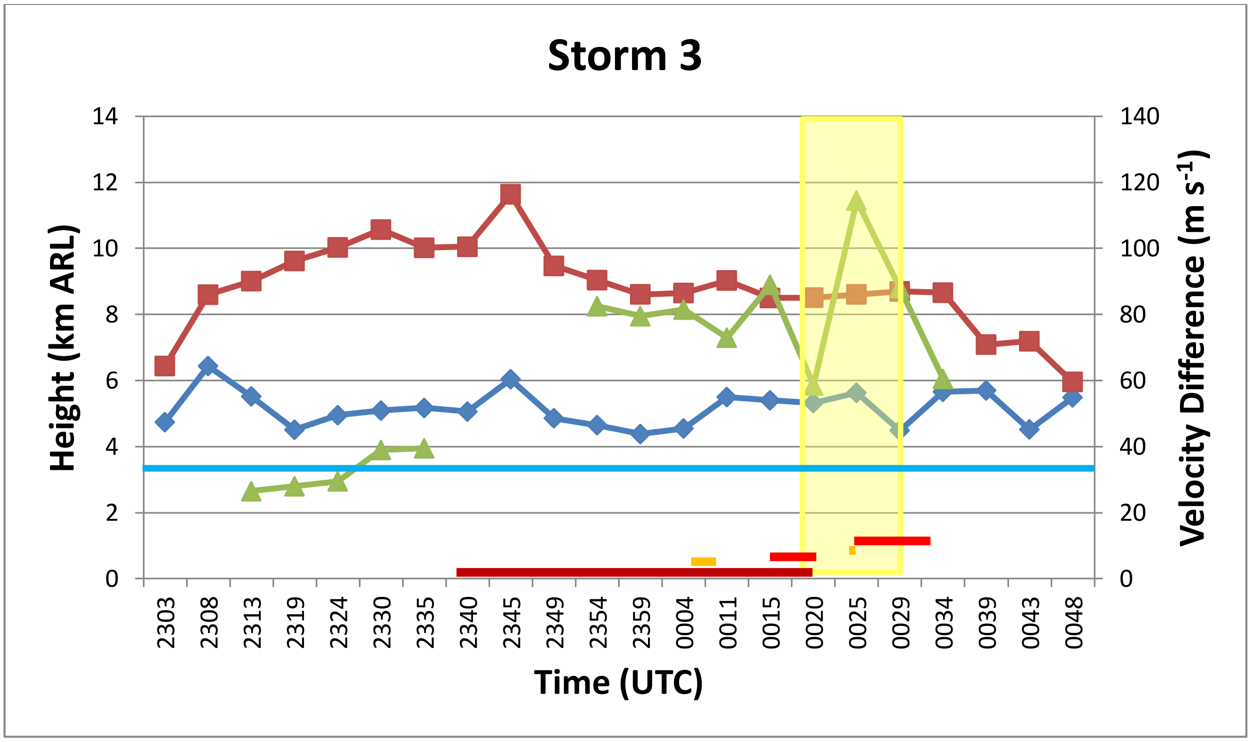

Fig. 6. Maximum height of 60 dBZ Z_{HH} (red line with squares) and top of the 1-dB Z_{DR} column (blue line with diamonds) with maximum velocity difference (green line with triangles, m s^{-1}). Horizontal, light blue line marks approximate ambient 0°C height. Horizontal lines at the bottom are tornado reports with dark red representing the EF-4 tornado, bright red lines are EF-1 tornadoes, and orange lines are EF-0 tornadoes. The 6th tornado (also EF-1) occurred just after the end of this timeline from 0050-0051 UTC. Yellow box is approximate window of storm-boundary interaction.

approached the surface front. A Z_{DR} arc was briefly present from 2257 through 2308, but then disappeared for an extended period of time. There was no organized Z_{DR} arc visible from either KDVN or KLOT from 2313 through 0004. The Z_{DR} arc reappeared just before Storm 3 crossed the front, and was present most of the time from 0011 through 0029. As with Storms 1 and 2, appearance of the Z_{DR} arc may have represented a change in the storm-relative wind in the vicinity of the front.

Unlike Storms 1 and 2, there was no clear trend in maximum velocity difference across the mesocyclone. This may in part have been due to the measurement being applied to the low-level mesocyclone in Storm 3, while Storms 1 and 2 did not produce low-level mesocyclones.

4. DISCUSSION AND CONCLUSIONS

In the case of the 9 April 2015 anticyclonic supercells that crossed the surface quasi-stationary frontal boundary, the severe and near-severe hail reports were clustered around the time and geographic location where the storms interacted with the front. Both supercells also experienced a reduction in intensity, with Storm 1 temporarily regaining strength afterward and Storm 2 collapsing altogether. Storm 3 did not have an obvious change in intensity but may have changed modes in tornado production from a single, violent, long-track tornado to several successive weak, short-track tornadoes. All three supercells experienced substantial changes in Z_{DR} arc structure, with Storm 3 rapidly developing a Z_{DR} arc as it approached the surface front. The Z_{DR} arcs in Storms 1 and 2 broadened and mean Z_{DR} values appeared to increase as they crossed the front. Differences in storm-relative wind as the storms interacted with the boundary may have produced the observed changes in the storms' Z_{DR} arcs.

It is not possible to directly attribute the observed changes in storm structure and behavior to their interaction with the frontal boundary from these observations alone. It may be helpful to quantify Z_{DR} arc values in each supercell as they interact with the boundary to see how significant the observed evolution was. Obtaining and analyzing other cases of boundary-crossing supercells is also planned.

Acknowledgements: MVDB acknowledges UNL for providing regular academic year support.

References

Maddox, R. A., L. R. Hoxit, and C. F. Chappell, 1980: A study of tornadic thunderstorm interactions with thermal boundaries. *Mon. Wea. Rev.*, **108**, 322-336.

Markowski, P. M., E. N. Rasmussen, and J. M. Straka, 1998: The occurrence of tornadoes in supercells interacting with boundaries during VORTEX-95. *Wea. Forecasting*, **13**, 852-859.

Rasmussen, E. N., S. Richardson, J. M. Straka, P. M. Markowski, D. O. Blanchard, 2000: The association of significant tornadoes with a baroclinic boundary on 2 June 1995. *Mon. Wea. Rev.*, **128**, 174-191.

Rogash, J. A., and R. D. Smith, 2000: Multiscale overview of a violent tornado outbreak with attendant flash flooding. *Wea. Forecasting*, **15**, 416-431.

Weaver, J. F. and S. P. Nelson, 1982: Multiscale aspects of thunderstorm gust fronts and their effects on subsequent storm development. *Mon. Wea. Rev.*, **110**, 707-718.